Journal of Solid State Chemistry 228 (2015) 105–109

Contents lists available at ScienceDirect

Journal of Solid State Chemistry

journal homepage: www.elsevier.com/locate/jssc

The effect of Ba-site substitution on the magnetic behavior of ordered perovskite $RBaMn_2O_6$ (R = rare earth)

Daisuke Akahoshi*, Daiki Iijima, Toshiaki Saito

Department of Physics, Faculty of Science, Toho University, Funabashi, Chiba 274-8510, Japan

ARTICLE INFO

Article history:
Received 5 February 2015
Received in revised form
16 April 2015
Accepted 17 April 2015
Available online 25 April 2015

Keywords:
Perovskite manganite
Chemical substitution
Structural randomness
Magnetic transitions

ABSTRACT

We have investigated the effect of Ba-site substitution with *Ae* (*Ae* = Sr and Ca) on the magnetic properties of *A*-site ordered $RBaMn_2O_6$ with R = Pr, Nd, and $Nd_{0.5}Sm_{0.5}$. Ba-site substitution reduces the mismatch between the average ionic radii of *R*- and Ba-sites, but introduces structural randomness into Ba-site. A reduction in the *R*/Ba mismatch suppresses the charge/orbital ordered insulating (COOI) state of $Nd_{0.5}Sm_{0.5}BaMn_2O_6$ and the A-type antiferromagnetic (AAF) one of $PrBaMn_2O_6$, while the Curie temperature of $PrBaMn_2O_6$ is almost insensitive to Ba-site substitution. At the multicritical point where the COOI, AAF, and ferromagnetic metallic (FM) states meet, the effect of the structural randomness is dominant; with increasing the structural randomness, the FM and AAF transition temperatures of $NdBaMn_2O_6$ decrease.

1. Introduction

Perovskite manganites $R_{1-x}Ae_xMnO_3$ (R = rare earth, *Ae* = alkaline earth) have been attracting much interest because of their colossal magnetoresistance (CMR) and potential application in magnetic devices such as magnetic sensor [1,2]. Among many perovskite manganites, $RBaMn_2O_6$ is one of the candidate materials for such magnetic devices, because both the ferromagnetic metallic (FM) and charge/orbital ordered insulating (COOI) phases, which are indispensable for the CMR effect, show up above room temperature [3–7]. The crystal structure and electronic phase diagram of $RBaMn_2O_6$ are shown in Fig. 1. $RBaMn_2O_6$ has the *A*-site ordered perovskite structure in which *R*O and BaO layers are alternately stacked along the *c*-axis. *R*/Ba order is caused by the large mismatch between the ionic radii of R^{3+} and Ba^{2+} (*R*/Ba mismatch). $RBaMn_2O_6$ with R = Sm–Dy, and Y have the COOI ground state, and the COOI transition temperature T_{CO} reaches 500 K at R = Y [4]. On the other hand, $RBaMn_2O_6$ with R = Pr and Nd exhibit successive magnetic transitions; the FM transition occurs above room temperature, and then the A-type antiferromagnetic (AAF) transition does below the Curie temperature T_C. As seen from the phase diagram, the COOI, FM, and AAF orders coincide with each other around room temperature to form a multicritical point at R = Nd [5–7].

Around the multicritical region, chemical substitution of Ba-site with heterovalent R^{3+}, which corresponds to electron-doping, drastically changes the magnetic and transport properties of $RBaMn_2O_6$ [8,9]. In the case of $NdBaMn_2O_6$, partial substitution of Ba^{2+} with Nd^{3+} creates FM domains in the AAF matrix, and as a result of 5%–substitution, the FM domains are dominant [9]. Nakajima et al. reported that $RBa_{1-x}La_xMn_2O_6$ (R = $Sm_{0.90}La_{0.10}$, x = 0.14) exhibits the CMR effect at room temperature [8]. These results indicate that elaborate investigation of the effect of Ba-site substitution might provide crucial keys for realizing new magnetic devices using the CMR effect. To our knowledge, the effect of substitution of Ba-site with isovalent *Ae* (*Ae* = Sr^{2+} and Ca^{2+}), which corresponds to band-width control, has not been systematically studied yet. In this study, we have prepared $RBa_{1-x}Ae_xMn_2O_6$ (R = Pr, Nd, and $Nd_{0.5}Sm_{0.5}$, x = 0, 0.05, and 0.10), and investigated their magnetic properties.

2. Experimental

$RBa_{1-x}Ae_xMn_2O_6$ in polycrystalline form were prepared by a solid state reaction. We employed Pr_6O_{11}, Nd_2O_3, Sm_2O_3, $BaCO_3$, $CaCO_3$, $SrCO_3$, and Mn_3O_4 as starting materials. Mixed powders with appropriate molar ratio were pressed into the pellets, and sintered at 1523 K under Ar atmosphere. Then, we annealed these sintered samples under O_2 flow to obtain oxygen-stoichiometric samples. We could not obtain single phase samples of $RBa_{1-x}Sr_xMn_2O_6$ with $x > 0.1$ and $RBa_{1-x}Ca_xMn_2O_6$ with $x > 0.05$. This might be due to site-mixing between R^{3+} and dopant Ae^{2+}. Magnetic properties were studied using a Quantum Design

* Corresponding author. Tel.: +81 47 472 5922; fax: +81 47 472 5925.
E-mail address: daisuke.akahoshi@sci.toho-u.ac.jp (D. Akahoshi).

http://dx.doi.org/10.1016/j.jssc.2015.04.020
0022-4596/

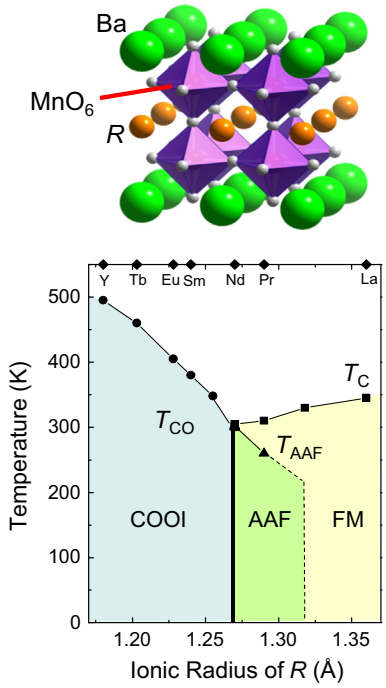

Fig. 1. Crystal structure and electronic phase diagram of RBaMn$_2$O$_6$. T_{CO}, T_C, and T_{AAF} denote charge/orbital ordered insulating (COOI), ferromagnetic metallic (FM), and A-type antiferromagnetic (AAF) phase transition temperatures, respectively.

magnetic property measurement system (MPMS). Sample characterization was performed by powder X-ray diffraction (XRD) methods using Cu$K\alpha$ radiation at room temperature.

3. Results and discussion

Fig. 2 shows the XRD patterns of RBa$_{1-x}Ae_x$Mn$_2$O$_6$ with (a) R = Pr, (b) Nd, and (c) Nd$_{0.5}$Sm$_{0.5}$. Structural analysis indicates that all the samples prepared in this study have A-site ordered perovskite structure and are free of impurity phases [10]. The (001) reflection around $2\theta = 11.5^\circ$, which arises from the alternate stack of RO and BaO layers, is a piece of evidence for A-site cation order, and this reflection is clearly observed in the XRD patterns of all the samples (the insets of Fig. 2). Both PrBa$_{1-x}Ae_x$Mn$_2$O$_6$ and NdBa$_{1-x}Ae_x$Mn$_2$O$_6$ have the orthorhombic structure with a space group of $Pmmm$ and a unit cell of $a_p \times a_p \times 2a_p$ at room temperature. Here a_p denotes a lattice parameter in a simple cubic perovskite setting. On the other hand, Nd$_{0.5}$Sm$_{0.5}$Ba$_{1-x}Ae_x$Mn$_2$O$_6$, which has the COOI state at room temperature, crystallizes in the pseudo-tetragonal structure with a space group of $P4/mmm$ and a unit cell of $a_p \times a_p \times 2a_p$. Morikawa et al. recently reported that the COOI RBaMn$_2$O$_6$ (R = Sm) has the orthorhombic structure with a space group of $Pnam$ ($2\sqrt{2}a_p \times \sqrt{2}a_p \times 4a_p$) at room temperature [11]. However, in this study, for simplicity, the XRD profiles of Nd$_{0.5}$Sm$_{0.5}$Ba$_{1-x}Ae_x$Mn$_2$O$_6$ are indexed as the pseudo-tetragonal structure. The refined lattice parameters are listed in Table 1.

The orthorhombic or tetragonal lattice distortion of RBaMn$_2$O$_6$ is caused by the large R/Ba mismatch. Thus, substitution of Ba^{2+} with a smaller cation such as Ca^{2+} and Sr^{2+} is expected to relax the lattice distortion caused by the R/Ba mismatch (the ionic radii of Ba^{2+}, Sr^{2+}, Ca^{2+}, and R^{3+} are 1.61 Å, 1.44 Å, 1.34 Å, and 1.18–1.36 Å, respectively). As expected, with increasing Sr-doping level, the lattice distortion, defined as $(a+b)/c$ in this study, is being relaxed, that is, $(a+b)/c$ is approaching unity (Table 1). Ca-substitution also relaxes the lattice distortion as in the case of Sr-substitution.

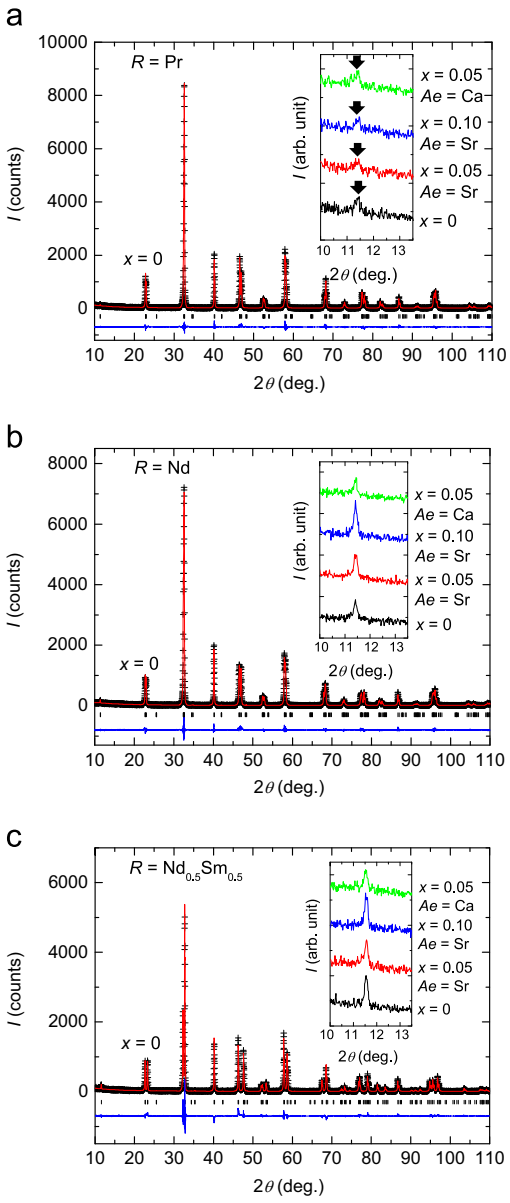

Fig. 2. Rietveld refined X-ray diffraction profiles of RBa$_{1-x}Ae_x$Mn$_2$O$_6$ (Ae = Sr and Ca) with (a) R = Pr, (b) Nd, (c) Nd$_{0.5}$Sm$_{0.5}$ at room temperature.

Fig. 3(a) and (b) shows the temperature (T) dependence of the zero-field-cooled (ZFC) magnetization (M) for PrBa$_{1-x}$Sr$_x$Mn$_2$O$_6$ (Pr–Sr) and PrBa$_{1-x}$Ca$_x$Mn$_2$O$_6$ (Pr–Ca) at H = 1 kOe. As mentioned above, PrBaMn$_2$O$_6$ exhibits the successive magnetic transitions; the M shows an abrupt increase at $T_C = 305$ K, and then suddenly drops at the AAF transition temperature $T_{AAF} = 260$ K with a thermal hysteresis. In this study, the T_C's of RBa$_{1-x}Ae_x$Mn$_2$O$_6$ (R = Pr and Nd) are determined from the Curie–Weiss fitting. With increasing Sr-concentration, the T_{AAF} is monotonously decreasing from 260 K ($x = 0$) to 254 K ($x = 0.05$) then to 246 K ($x = 0.10$). In the case of Pr–Ca with x = 0.05 (Fig. 3(b)), at first glance, the T_{AAF} seems to be same as that of Pr–Sr with $x = 0.10$. However, as seen from the derivative of the M (dM/dT) (the inset of Fig. 3(b)), the abrupt change in the M of Pr–Ca with $x = 0.05$ starts at $T_{AAF} = 250$ K, which is higher than that of Pr–Sr with $x = 0.10$ ($T_{AAF} = 246$ K) but lower than that of Pr–Sr with $x = 0.05$ ($T_{AAF} = 254$ K). On the other hand, the T_C is not so susceptible to Ba-site substitution. The T_C's of Pr–Sr with x = 0.05, 0.10, and Pr–Ca with x = 0.05 are 305 K, 304 K, and 303 K, respectively. These values almost coincide with that of the